

Break of universality for an Ising model with aperiodic Rudin-Shapiro interactions

R.F.S. Andrade^a and S.T.R. Pinho

Instituto de Física, Universidade Federal da Bahia, Campus da Federação, 40210-340 Salvador, Brazil

Received 18 December 2002 / Received in final form 27 February 2003

Published online 11 August 2003 – © EDP Sciences, Società Italiana di Fisica, Springer-Verlag 2003

Abstract. We analyze the ferromagnetic Ising model on non-Euclidean scale invariant lattices with aperiodic interactions (J_A, J_B, J_C, J_D) defined by Rudin-Shapiro substitution rules with Migdal-Kadanoff renormalization (MKR) and transfer matrix (TM) techniques. The analysis of the invariant sets of the zero-field MKR transformation indicates that the critical behavior, completely distinct from the one of the uniform model, is described by a new off-diagonal fixed point. This contrasts with other aperiodic models where the new critical behavior is described by a period-two cycle. With the new fixed point, values for the thermal critical exponents, α and ν , as well as the period of log-periodic oscillations, are obtained. Exact recursive maps for all thermodynamical functions are derived within the TM approach. The explicit dependence of the thermodynamical functions with respect to temperature is evaluated by the numerical iteration of the set of maps until a previously chosen convergence is achieved. They also indicate that, depending on the actual choice for the aperiodic coupling constants, the magnetic exponents (β and γ) assume different values. However the Rushbrook relation is always satisfied.

PACS. 05.50.+q Lattice theory and statistics – 05.10.Cc Renormalization group methods – 64.60.Ak Renormalization-group, fractal, and percolation studies of phase transitions – 61.44.Br Quasicrystals

1 Introduction

Spin models with aperiodic interactions can be deterministically constructed with a proper substitution rule for a finite set of symbols (or letters) in subsequent steps [1]. Deterministic aperiodicity may be introduced into the model by using different coupling interactions between the spins according to the order of symbols in such a sequence [2], much in the way that was adopted with success for the analysis of electronic systems [3].

The investigation of the critical behavior of deterministic aperiodic models uses Luck's criterion for relevant or irrelevant fluctuations [4]. According to this formulation, relevant fluctuations in the values of the coupling constants bring the aperiodic system out of the universality class defined by the uniform one. This is caused by structural instability of the renormalization flow in the original parameter space with respect to the new dynamics imposed on an enlarged space by the aperiodic sequence. The critical properties are then described by new invariant sets in the new parameter space.

In a previous work [5], one of us investigated some preliminary aspects of an aperiodic Ising model induced by the four letter Rudin-Shapiro sequence within a MKR approach. This sequence plays a singular role in the anal-

ysis of aperiodic systems as its wandering exponent Ω , the value of which is related to the structural stability of the invariant sets, is equal to the one obtained for the fully random situation. According to that analysis, fluctuations induced by the RS sequence are *relevant*, so that the critical properties differ from those of the uniform system.

The purpose of this work is to present a detailed analysis of this system, addressing both the structure of its renormalization flow in the parameter space as well as the thermodynamical properties. Values for the specific heat and correlation exponents, α and ν , and the frequency of the log-periodic oscillations ω that are observed in the vicinity of the critical temperature are obtained after the identification of the invariant sets and their stability properties within MKR approach. They can also be evaluated from the corresponding thermodynamical quantities in the neighborhood of the critical point, which are obtained from the TM recurrence relations. This procedure uncovered a new result: the break of universality of the magnetic exponents β and γ , which become dependent of the relative strength of the four coupling constants.

The behavior of aperiodic systems is very sensitive to the introduction of disturbances and averages in the sequence that generates the aperiodicity, as occurs in most perturbation approaches. On the other hand, it is virtually impossible to exactly treat such systems on Euclidean

^a e-mail: randrade@ufba.br

systems. As the main issue of this work is to accurately describe the influence of aperiodicity, we are forced to resort to other strategies, where this effect can exactly be dealt with. The one adopted in this work is to insert aperiodicity into the scale invariant Diamond Hierarchical Lattices (DHL). Models on these structures undergo phase transitions, so that the effect of aperiodicity on the critical behavior can be analyzed. Such lattices are not physically realizable but, as they can be regarded as a MKR approximation to Euclidean lattices, the results obtained herein are relevant to uncover the behavior of aperiodic actual systems.

The rest of the work is organized as follows: In Section 2 we present a brief discussion of our model. In Section 3 we present the MKR formulation of the problem and discuss the results produced for the exponents α and ν and the frequency ω of log-periodic oscillations. We also discuss the new invariant sets and flow in parameter space. In Section 4 we discuss the main steps for formulation of the problem in the TM formalism. In Section 5 we present the results produced by the recurrence maps. The exponents α and ν agree with the values from MKR, but the frequency ω misses a factor 2. In this section we also discuss the results that indicate the break of universality of the magnetic exponents observed within the TM approach. Finally, Section 6 closes with concluding remarks.

2 Rudin-Shapiro sequence and Ising models

The Rudin-Shapiro aperiodic 4-letter sequence is based on the following substitution or inflation rule:

$$\begin{aligned} A &\rightarrow AC, & B &\rightarrow DC, \\ C &\rightarrow AB, & D &\rightarrow DB. \end{aligned} \quad (1)$$

The usual choice is to set up the zero-th order generation to letter A . In order to provide a concise notation for the models constructed with the help of Rudin-Shapiro sequence, it is useful to define the maps $\mu(\ell)$ and $\zeta(\ell)$ as, respectively, the first and second letters of the inflation rule (1), namely

$$\begin{aligned} \mu(A) = \mu(C) = A, & \quad \mu(B) = \mu(D) = D, \\ \zeta(A) = \zeta(B) = C, & \quad \zeta(C) = \zeta(D) = B. \end{aligned} \quad (2)$$

The substitution matrix \mathbf{M} of a sequence relates the number of symbols in two subsequent steps. For the Rudin-Shapiro rule,

$$\mathbf{M} = \begin{pmatrix} 1 & 0 & 1 & 0 \\ 0 & 0 & 1 & 1 \\ 1 & 1 & 0 & 0 \\ 0 & 1 & 0 & 1 \end{pmatrix}, \quad (3)$$

and its eigenvalues are $\lambda_1 = 2$, $\lambda_{2,3} = \pm\sqrt{2}$, $\lambda_4 = 0$. The wandering exponent

$$\Omega = \frac{\log |\lambda_2|}{\log \lambda_1} = \frac{1}{2}, \quad (4)$$

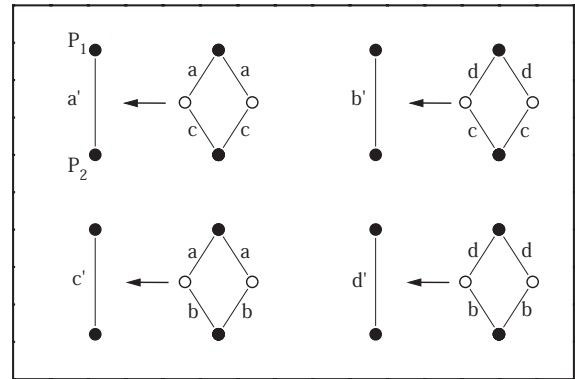


Fig. 1. Basic graphs to set up the MKR transformation for an Ising model on a DHL with $p = 2$ branches whose coupling constants J_ℓ , $\ell = A, B, C, D$ are defined by Rudin-Shapiro inflation rule (1). The decimation procedure follows the corresponding deflation rule $\mu(\ell) \zeta(\ell) \rightarrow \ell$ where $\mu(\ell)$ and $\zeta(\ell)$ are given by (6). P_1 and P_2 are the root sites of DHL.

assumes the value required to satisfy Harris criterion, according to which the presence of random disorder on spin models with $\omega \geq 1/2$ may change its critical behavior.

Luck's work extends, in a heuristic approach, Harris criterion to aperiodic systems. An exact version of this criterion for DHL's has been presented in reference [6]. It states that relevant fluctuations, *i.e.*, those for which

$$\Omega > \Omega_c = 1 - \frac{1}{\nu} = 1 - \frac{d_f}{2 - \alpha}, \quad (5)$$

do cause a change in the critical properties.

For the present investigation we adopt a formal Hamiltonian

$$\mathcal{H} = - \sum_{(i,j)} J_{ij} \sigma_i \sigma_j - h \sum_i \sigma_i. \quad (6)$$

$\sigma_i = \pm 1$ are Ising spin variables placed on each site of the DHL, interacting only with their first neighbors, as indicated by the notation (i, j) . To fix the investigation of aperiodicity in a square lattice, let us consider an axial direction so that J_{ij} vary only along it, keeping the system invariant along transverse direction. In order to focus on the exact effect of aperiodicity, we consider the system within the MKR scheme.

The MKR on a square lattice consists to successively reducing basic cells to a single bond linking to root sites, but it can be better explained with the help of DHL's [7, 8]. These are recursively constructed from an initial unit, a line segment, and a geometrical rule, indicating how the elements present therein will be replaced in any further steps of its construction (see Fig. 1): replace each bond by a unit cell with p branches, each of them formed by b bonds linking $b-1$ new inner sites. The fractal dimension for such lattice is

$$d_f = \frac{\log(pb)}{\log(b)}. \quad (7)$$

In the present work we consider the most simple case, $b = p = 2$, so that $d_f = 2$. We identify the DHL's by the

number G (for generation), which counts the number of times that the rule has been applied. $G = 0$ corresponds to a single segment linking the two root sites. For any G , the number of bonds is $N_{G,B} = 4^G$, the number of sites is $N_{G,S} = 2(2 + 4^G)/3$, the number of bonds in any of the shortest paths linking the two root sites is $N_{G,P} = 2^G$, that is also equal to the number of distinct paths. The magnetic system is constructed by placing an Ising spin in each DHL site, interacting with all of its nearest neighbors.

To consider the Rudin-Shapiro aperiodicity, the coupling constants J_{ij} assume only 4 distinct values. Their site dependent value are precisely defined: start from one of the root sites, and assign sequentially $J_{ij} = J_\ell$, $\ell = A, B, C$ or D according to the sequence of letters emerging from the recursive application of (1). Restricting to the situation of axial modulation, the system becomes aperiodic only along the paths between the root sites, while all paths are constituted by the same sequences of bonds. The external uniform field h is the same for all sites of the lattice, independent on its local coordination.

3 Invariant sets and flows in parameter space

The geometrical growth process used in the construction of DHL's leads to exact scale invariant objects. When we consider physical models defined on such structures, the decimation procedure used in MKR formalism proceeds in the opposite way to the growth process. Hence, the maps linking the coupling parameters in two successive decimation steps are also exact, so that critical properties of the model under investigation can be precisely investigated. In the case of a uniform model in zero-field case, a single map results from the use of the MKR formalism. For the present model, a set of four maps is required to account for the four distinct coupling constants induced by the Rudin-Shapiro rule (1). So let us define

$$x_\ell = \tanh[\beta J_\ell], \quad \ell = A, B, C, D. \quad (8)$$

The recursion relations in terms of these variables read

$$x'_\ell = \frac{2x_{\mu(\ell)}x_{\zeta(\ell)}}{1 + x_{\mu(\ell)}^2x_{\zeta(\ell)}^2}, \quad \ell = A, B, C, D. \quad (9)$$

The critical properties of the model are defined by the invariant sets of equations (9). Two of them are the two trivial fixed points, FPI and FPO , with coordinates $(0, 0, 0, 0)$ and $(1, 1, 1, 1)$, which correspond to the uniform paramagnetic and ferromagnetic states at, respectively, $T = \infty$ and $T = 0$. A non-trivial uniform fixed point (UFP), lying in the hypercube diagonal, whose coordinates

$$x_\ell = \frac{1}{3} \left[-1 + \frac{(17 + \sqrt{297})^{2/3} - 2}{(17 + \sqrt{297})^{1/3}} \right] = 0.543689\dots, \quad \ell = A, B, C, D, \quad (10)$$

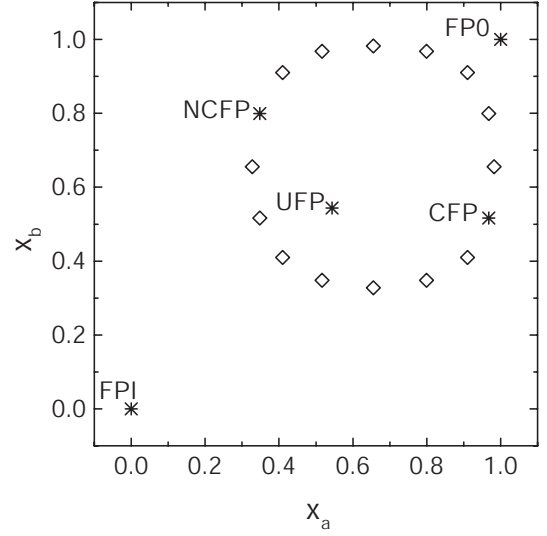


Fig. 2. The projection of the invariant sets onto the plane (x_A, x_B) of the parameter space of the Ising model on a DHL with interactions based on Rudin-Shapiro substitution rule. The five fixed points, represented by stars are identified by corresponding acronyms; and the seven distinct period-two cycles by diamonds.

are equal to the fixed point's coordinate of the uniform model, is obtained by the real positive solution of the equation

$$x^4 - 2x + 1 = 0. \quad (11)$$

The dynamics of the uniform model is restricted to the hypercube diagonal of the Rudin-Shapiro parameter space, which can be identified with the thermal direction. It is easy to prove that, for the Rudin-Shapiro aperiodic model, the linearized MKR transformation around the UFP results in

$$\vec{X}' = c\mathbf{M}^T\vec{X} \quad (12)$$

where \vec{X} indicates the vector of components x_ℓ , $\ell = A, B, C, D$, $c = 0.839286$ and \mathbf{M}^T is the transpose of \mathbf{M} defined by equation (3). In the uniform case, this unstable fixed point has one single eigenvalue $\Lambda_1 = c\lambda_1 > 1$. The flow defined by $c\mathbf{M}^T$ is characterized by three unstable directions, as $|\Lambda_{2,3}| > 1$. There is a super stable direction, corresponding to the fourth eigenvector $\Lambda_4 = 0$. We call it super stable as any component of the flow along this direction shrinks to zero in a single step.

The critical set for this model must have one single unstable eigenvalue, corresponding to the thermal eigenvector, as the other eigenvalues reflect geometrical properties of the Rudin-Shapiro sequence. Thus we looked for further fixed points and period-two cycles. This root finding problem, that can not be solved analytically, has been carried out with the help of both algebraic and numerical programs. We have found two further fixed points, seven period-two cycles, the projection of which onto the plane (x_A, x_B) is shown in Figure 2. Their coordinates form rather symmetric figures in most of the planes where they can be projected. The figure also suggests that the

Table 1. The coordinates of the non-diagonal invariant sets of the model: 7 period-two cycles $C_{n,i}$, $n = 1, \dots, 7$ and $i = 1, 2$, and 2 fixed points, $NCFP$ and CFP .

Cycle	x_a	x_b	x_c	x_d
$C_{1,1}$	0.4102	0.91054	0.4102	0.91054
$C_{1,2}$	0.32727	0.65556	0.65556	0.98269
$C_{2,1}$	0.91054	0.4102	0.91054	0.4102
$C_{2,2}$	0.98269	0.65556	0.65556	0.32727
$C_{3,1}$	0.91054	0.91054	0.4102	0.4102
$C_{3,2}$	0.65556	0.32727	0.65556	0.98269
$C_{4,1}$	0.4102	0.4102	0.91054	0.91054
$C_{4,2}$	0.65556	0.98269	0.65556	0.32727
$C_{5,1}$	0.79965	0.9681	0.34764	0.51609
$C_{5,2}$	0.51609	0.34764	0.9681	0.79965
$C_{6,1}$	0.79965	0.34764	0.9681	0.51609
$C_{6,2}$	0.9681	0.79965	0.51609	0.34764
$C_{7,1}$	0.34764	0.51609	0.79965	0.9681
$C_{7,2}$	0.51609	0.9681	0.34764	0.79965
$NCFP$	0.34764	0.79965	0.9681	0.51609
CFP	0.9681	0.51609	0.79965	0.34764

two non-diagonal fixed points could form a two-cycle, completing the ellipse where the fourteen points belonging to the seven two-cycles lie. Table 1 indicates that all 64 coordinates of the cycles $C_{n,j}$ and non-diagonal fixed points are selected from only 9 different values.

All of the seven period-two cycles have three unstable eigenvalues $|A| > 1$ and a super stable $A_4 = 0$. The two non diagonal fixed points have different properties. There is a non critical fixed point ($NCFP$), with coordinates

$$(x_A, x_B, x_C, x_D) = (0.34764, 0.79965, 0.96810, 0.51609), \quad (13)$$

and eigenvalues $\Lambda_1 = 1.79506$, $\Lambda_2 = 1.3877$, $\Lambda_3 = -0.82865$, and $\Lambda_4 = 0$. Finally the critical fixed point (CFP), with coordinates

$$(x_A, x_B, x_C, x_D) = (0.96810, 0.51609, 0.79965, 0.34764), \quad (14)$$

has the correct spectrum expressed by $\Lambda_1 = 1.58655$, $\Lambda_2 = -0.99955$, $\Lambda_3 = 0.601187$ and $\Lambda_4 = 0$. As we will show in the next sections, all physical properties related to the CFP are corroborated by the explicit evaluations within the TM approach.

Note that one vanishing eigenvalue is present in the spectra for all investigated invariant sets of this model. This is related to the fact that, if $A = D$ and $B = C$, the resulting sequence is periodic, as all symbols are mapped onto a single group, *i.e.*,

$$A, B, C, D \rightarrow AB. \quad (15)$$

This is the direction of the eigenvector corresponding to λ_4 . Thus, Rudin-Shapiro modulated spin models with values for the coupling constants taken along this particular direction have the same critical behavior as the uniform model.

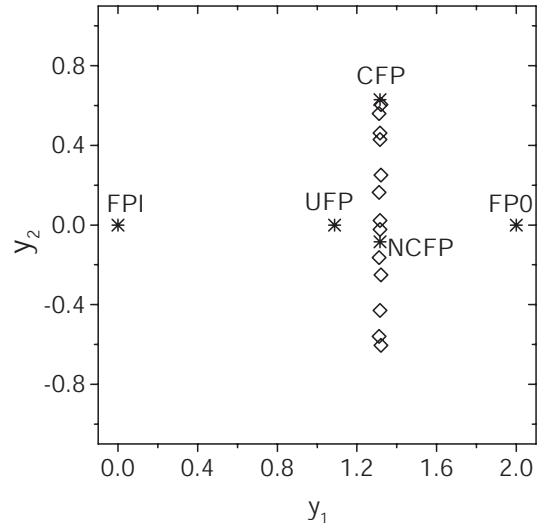


Fig. 3. The projection of the invariant sets (shown in Fig. 2) onto the plane (y_1, y_2) of the parameter space expressed in terms of the new variables y_n , $n = 1, \dots, 4$.

In order to set up the critical manifold, we take advantage of this super-stable direction for the analysis of the flow in parameter space. We use

$$\Gamma = \frac{1}{2} \begin{pmatrix} 1 & 1 & 1 & 1 \\ 1 & 1 - \sqrt{2} & 1 + \sqrt{2} & -1 \\ 1 & \sqrt{2} - 1 & -1 - \sqrt{2} & -1 \\ 1 & -1 & -1 & 1 \end{pmatrix}, \quad (16)$$

constructed with the eigenvectors of \mathbf{M} , to define new variables $y_n = (\Gamma)_{nl}^{-1} x_l$. In the same way, we can transform the coupling constants (J_A, J_B, J_C, J_D) to a Γ defined basis (J_1, J_2, J_3, J_4) . In this new basis, the coordinates of the quoted fixed points are:

$$\begin{aligned} FPI &: (0, 0, 0, 0); & FPO &: (2, 0, 0, 0); \\ UFP &: (1.08738, 0, 0, 0); \\ CFP &: (1.31574, 0.62985, -0.00939, 0); \\ NCFP &: (1.31574, -0.08423, -0.08423, -0.45201). \end{aligned} \quad (17)$$

Figure 3 illustrates the projection of the invariant sets in the plane (y_1, y_2) .

The evaluation of the critical exponents [10] based on the eigenvalues of the CFP leads to:

$$\nu = \frac{\ln 2}{\ln \Lambda_1} = 1.50174; \quad \alpha = 2 - 2\nu = -1.00349. \quad (18)$$

As expected, the resulting values differ from those for the uniform system, confirming that the fluctuations in the coupling constants induced by the Rudin-Shapiro sequence are *relevant*.

A well known formal solution to the MKR equations states that scaling part of the free energy behaves like

$$f(t) = |t|^{2-\alpha} P \left(\frac{\log_{10} |t|}{\log_{10} \Lambda_1} \right), \quad (19)$$

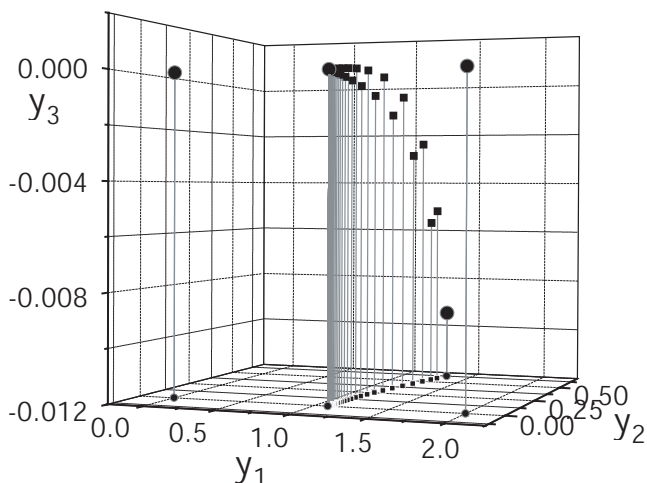


Fig. 4. One orbit (squares) of the renormalization flow projected in the hyperplane (y_1, y_2, y_3) of the parameter space expressed in terms of the transformed variables y_n , $n = 1, \dots, 4$. This orbit, that leaves the neighborhood of *CFP*, is constrained to the manifold linking *CFP* to *UFP*. The positions of *FPI*, *FP0*, *CFP* and *UFP* are indicated by full circles.

where Λ_1 is the unstable thermal eigenvalue of the renormalization flow close to the critical fixed point (or other critical set), t is the reduced temperature $t = |T - T_c|/T_c$ and P is a periodic function with period 1. This includes the possibility $P = \text{constant}$, what is actually verified in a large number of cases. For systems with discrete scale invariance, as in the case of DHL and other fractal lattices, P may actually oscillate [11]. For the value $\Lambda_1 = 1.58655$ obtained for the *CFP*, we find the frequency ω of log-periodic oscillations as

$$\omega = \frac{2\pi}{\log_{10}\Lambda_1} = 31.34481\dots \quad (20)$$

Now we focus on the renormalization flow in parameter space. With exception of *NCFP*, all other fixed points lie on the $y_4 = 0$ plane. We illustrate, in Figure 4, their position in the sub-space spanned by the axes (y_1, y_2, y_3) . For all fixed points, the thermal eigenvector points along the y_1 axis and, in the uniform case, the flow is restricted to this axis, where the *UFP* and the two trivial fixed points lie. When different values for the coupling constants are considered, the flow leaves this axis and meanders in the three dimensional space. Trajectories leaving the neighborhood of *UFP* feel the attraction of the *CFP* before being attracted to either of the trivial fixed points. The form of the trajectories suggests the presence of a higher than one-dimensional critical manifold linking the *UFP* to the *CFP*, where the renormalization critical dynamics occurs.

It is difficult to precisely define this manifold, while some of its geometrical properties can be obtained by tracing the loci of a large number of orbits leaving the *UFP*. However, as the *CFP* is also unstable, the trajectories deviate easily from the manifold. In order to circumvent this

problem [12], we have considered the inverse maps of (9), which read

$$x_{\mu(\ell)}x_{\zeta(\ell)} = \frac{1 - \sqrt{1 - x'_\ell{}^2}}{x'_\ell} \quad \ell = A, B, C, D. \quad (21)$$

Now we iterate (21), restricted to the condition $y_4 = x_A - x_B - x_C + x_D = 0$, starting from several points in the stable manifold close to *CFP* defined by (14). Upon iteration, the trajectories will be repelled from *CFP* in the direction of *UFP*, indicating more precisely the form of the critical manifold, as illustrated in Figure 4. Note that this manifold is more than one-dimensional since, for the inverse transformation, beside the super-stable direction, the *UFP* has three other stable directions, and the *CFP* has just another stable direction.

Before closing this section, we stress that the best value for the second eigenvalue of the *CFP* is indeed $\Lambda_2 = -0.99955$. This value was carefully investigated and, working with 16 digits variables in both Fortran and Mathematica codes, it does not come closer to the value -1 . This is a relevant issue as, if $\Lambda_2 = -1$, one of the flow directions in parameter space has the characteristics of a center manifold. In such cases, the character of the flow depends on second order terms. Within MKR framework, this is called a marginal value, which may lead to non-universal behavior depending on the nature of the infinitesimal perturbations like non-zero field. As we will discuss in the next section, the critical magnetic exponents, evaluated within the TM method, do depend on the values of the coupling constants. This may be related to this particular value for $\Lambda_2 \approx -1$, but, strictly speaking, we can not argue the presence of a marginal eigenvalue to explain this non-universal behavior.

4 Transfer matrix formulation

Although the MKR analysis reveals much of the critical behavior of the model, its whole characterization requires the knowledge of the free energy. For the present situation, this evaluation particularly important for the following reasons: i) we could only numerically locate the fixed point and higher order invariant sets of the MKR maps. Even with an exhaustive scanning for possible solutions, we can not disclose the existence of further fixed points and higher order cycles that could affect the critical behavior. We recall that, for other aperiodic systems [13], the criticality was found to be described by a two-cycle. ii) The value of Λ_2 for the *CFP* could raise doubts on whether it was actually responsible for the critical behavior. For DHL, the evaluation of the free energy can proceed within the same renormalization framework [14, 15]. In this work, the free energy is evaluated within the TM formulation, that also leads to the correlation length ξ , particularly useful for the identification of the critical point, due to its steep divergence at T_c .

DHL's are bounded by two root sites in any generation G . Thus, a 2×2 matrix \mathbf{T}_G is sufficient to describe all interactions present along the different paths that link

the two root sites. \mathbf{T}_G depends only on the 4 distinct states for the spins at the root sites, provided the contributions coming from all different configurations defined by the states of intermediate spins can be accounted for. The structure of \mathbf{T}_G , for the Rudin-Shapiro case, is similar to that one for the homogeneous system or for the aperiodic model induced by the double-period rule discussed in reference [16]. A matrix map, which expresses $\mathbf{T}_{G+1} = \mathbf{T}_{G+1}(\mathbf{T}_G)$ can be derived in a straightforward way, leading to a set of maps which expresses the matrix elements of \mathbf{T}_{G+1} in terms of those of \mathbf{T}_G . For the present case, four matrices $\mathbf{T}_{G,\ell}$, $\ell = A, B, C$ and D , are required for the description of all different configurations for any value of G .

The resulting maps are highly non linear and can be hardly integrated. However, they can be easily iterated on a computer, leading to numerically exact results for the thermodynamical functions per spin in the limit $G \rightarrow \infty$. To this purpose it is convenient to make a variable transformation, and write the set of maps in terms of the G -dependent free energy per spin $f_{G,\ell}$ and correlation length $\xi_{G,\ell}$. They are defined in terms of the eigenvalues of $\mathbf{T}_{G,\ell}$, $\eta_{G,\ell}$ and $\epsilon_{G,\ell}$ ($\eta_{G,\ell} \geq \epsilon_{G,\ell}$), $\ell = A, B, C, D$, as

$$f_{G,\ell} = -\frac{T}{N_{G,S}} \log \eta_{G,\ell},$$

$$\xi_{G,\ell} = N_{G,P} / \log(\eta_{G,\ell} / \epsilon_{G,\ell}). \quad (22)$$

In terms of these variables, the maps for the model with Rudin-Shapiro aperiodicity read:

$$f_{G+1,\ell} = 2 \frac{N_{G,S}}{N_{G+1,S}} (f_{G,\mu(\ell)} + f_{G,\zeta(\ell)})$$

$$- \frac{T}{N_{G+1,S}} \ln \left[\frac{1 + z_{G,\mu(\ell)}^2 z_{G,\zeta(\ell)}^2}{2} \right]$$

$$\xi_{G+1,\ell} = 2 \frac{\xi_{G,\mu(\ell)} \xi_{G,\zeta(\ell)}}{\xi_{G,\mu(\ell)} + \xi_{G,\zeta(\ell)}}$$

$$\times \left[1 + \frac{\xi_{G,\mu(\ell)} \xi_{G,\zeta(\ell)}}{\xi_{G,\mu(\ell)} + \xi_{G,\zeta(\ell)}} \ln \left(\frac{1 + z_{G,\mu(\ell)}^2 z_{G,\zeta(\ell)}^2}{2} \right) \right]^{-1}, \quad (23)$$

with

$$z_{G+1,\ell} = 2 \frac{z_{G,\mu(\ell)} z_{G,\zeta(\ell)}}{1 + z_{G,\mu(\ell)}^2 z_{G,\zeta(\ell)}^2}, \quad (24)$$

where

$$z_{G,\ell} = \exp(-N_{G,P} / \xi_{G,\ell}), \quad (25)$$

and $\mu(\ell)$, $\zeta(\ell)$, with $\ell = A, B, C, D$, are given by (2). Maps (23) are iterated starting from temperature dependent initial conditions, corresponding to the actual values of the functions in the $G = 0$ generation, where a single interaction J_ℓ between the root sites is present:

$$\eta_{0,\ell} = 2 \cosh(\beta J_\ell), \quad \epsilon_{0,\ell} = 2 \sinh(\beta J_\ell). \quad (26)$$

Other thermodynamical functions are obtained by deriving (23) with respect to the temperature, leading to

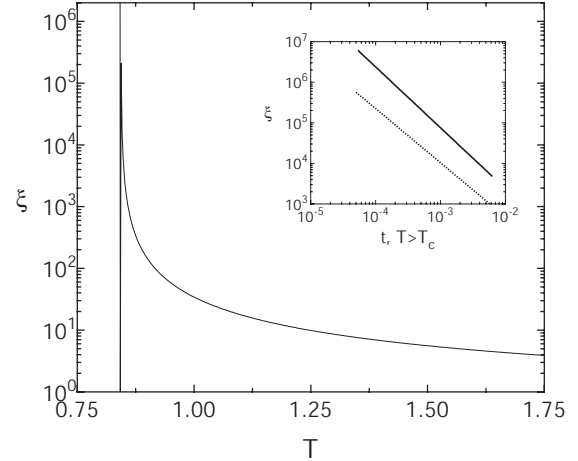


Fig. 5. Curve $\xi \times T$ for $(e_2, e_3, e_4) = (0.4, 0, 0)$. In the insert, curves $\log_{10}(\xi) \times \log_{10}(t)$, when $T > T_c$, for the non-uniform model $(0.4, 0, 0)$ (solid) and for the uniform model $(0, 0, 0)$ (dash).

maps for the entropy, $s_{G,\ell} = -\partial f_{G,\ell} / \partial T$ and specific heat $c_{G,\ell} = -T \partial^2 f_{G,\ell} / \partial T^2$. The enlarged set includes also maps for the derivatives of $z_{G,\ell}$. Finally, magnetization and susceptibility follow from maps for the derivatives of f_G with respect to the magnetic field. The corresponding maps for a two-letter aperiodic model have been explicitly indicated in reference [16].

The maps (23) are iterated with double precision FORTRAN variables until a very high relative precision (10^{-16}) is reached. Depending on the temperature, a number of $\sim 40-70$ iterations is required for this convergence, so that is quite reasonable to call the evaluation process as a numerical thermodynamical limit. Iterations were performed for a wide temperature interval. However, we concentrate our discussion to the T interval around the critical temperature T_c , where we can evaluate the critical exponents and other properties of the transition. The value for T_c can be obtained with, 16 digits precision, by the presence of a singular behavior in the numerical values for the thermodynamical functions, *e.g.*, in the behavior of $\xi(T)$: it has a well defined value for $T > T_c$, but it diverges for any $T < T_c$.

5 Thermodynamical behavior

To better discuss our results, it is convenient to use the transformed set of coupling constants J_i , $i = 1, 2, 3, 4$, as introduced in the Section 3. In order to define the contribution of the coupling constants, let $e_i = J_i / J_1$, $i = 2, 3, 4$. The discussion about the influence of the coupling constants on the critical behavior can be restricted to the space (e_2, e_3, e_4) .

Typical results for the behavior of ξ , for $(e_2, e_3, e_4) = (0.4, 0, 0)$ are shown in the Figure 5. In the insert we draw $\log_{10} \xi \times \log_{10} t$, for the same data and also for the uniform model $e_2 = e_3 = e_4 = 0$. The different critical behavior is expressed by different slopes.

Table 2. Results from the TM analysis for several choices of (e_2, e_3, e_4) the critical exponents β , γ , ν and α and the frequency ω were obtained fitting the data with the function (27).

	ϵ_2	ϵ_3	ϵ_4	β	γ	ν	α	$\alpha + 2\beta + \gamma$	ω
1	0	0	0	0.1617	2.3531	1.3383	-0.6765	2.0000	27.928
2	0	0	0.1	0.1617	2.3531	1.3383	-0.6765	2.0001	27.924
3	0	-0.1	0	0.0846	2.8342	1.5017	-1.0035	2.0000	-
4	0	0.1	0	0.0846	2.8342	1.5017	-1.0035	2.0000	15.673
5	0.4	0	0	0.1007	2.8022	1.5018	-1.0035	2.0000	-
6	0.1	0	0	0.1009	2.8016	1.5017	-1.0035	1.9999	-
7	-0.1	0	0	0.1009	2.8017	1.5017	-1.0035	2.0000	-
8	0.1	0.1	0.2	0.0854	2.8328	1.5018	-1.0036	1.9999	15.673
9	0.1	0.1	-0.2	0.0966	2.8104	1.5018	-1.0035	1.9999	15.673

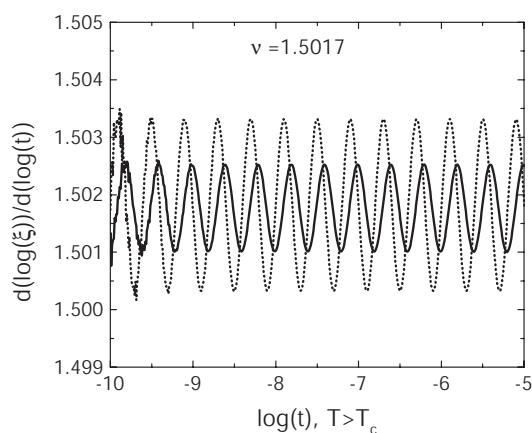


Fig. 6. Plots of $\frac{d(\log_{10}\xi)}{d(\log_{10}t)} \times \log_{10}t$ for two different values of (e_2, e_3, e_4) : $(0.4, 0, 0)$ (solid) and $(-0.1, 0.1, 0)$ (dot). The two curves oscillate about the same horizontal line, which equals the value of ν .

To better quantitatively analyze the obtained data for the different thermodynamical functions $g(t) = c, \xi, m, \chi$, we considered the derivatives $\mathcal{G} = \frac{d(\log_{10}g)}{d(\log_{10}t)}$, as function of $x = \log_{10}(t)$. Typical results, as those shown in Figure 6, suggest that the data can be fitted by the function

$$\mathcal{G}(x) = a + \frac{c}{x^d} + \sum_{n=1}^N b_n \cos(n\omega x + \phi_n). \quad (27)$$

The parameter c in (27) measures the distance from the data points to the actual scaling region in the neighborhood of T_c . When the points belong to the scaling region ($c \equiv 0$) the fit is expressed in terms of the critical exponent (a), the frequency ω , and the amplitudes and phases (b_n and ϕ_n) of the oscillatory function. Usually we obtain very good results for $N = 2$.

Results for several choices for (e_2, e_3, e_4) are summarized in the Table 2. The high quality of the procedure is attested by very low χ^2 values for all fittings (not shown). First note that the exponents for the periodic sequences obtained along the e_4 direction are the same as the uniform model (lines 1–2). Then, values for ν for any other

direction agree, with up to 5 significant digits, to that obtained within the MKR analysis (18), confirming that *CFP* actually describes the critical behavior. For distinct sets of coupling constants as shown in Figure 6, the corresponding functions \mathcal{G} have the same exponent, but differ from each other by the values for b_n and ϕ_n , *i.e.*, on the form of the periodic function P . The hyperscale relation, for independently evaluated values of α and ν is also confirmed with high precision. On the other hand, the value for ω is only the half of the one shown in (20). The discrepancy can be understood by considering the eigenvalue spectrum of the *CFP*: due to the presence of the negative eigenvalue Λ_2 , a trajectory in parameter space returns to the same side of a neighborhood of the *CFP* only after each two iterations of the MKR transformation, doubling the period of oscillation. This shows that the formal solution (19), which neglects the effect of other eigenvalues in the renormalization flow, is not complete and should be enlarged to coop with more complex situations.

Table 2 clearly shows that β and γ depend on the particular choice made for (e_2, e_3, e_4) , indicating a break of universality for the magnetic critical behavior of the model. This situation is completely distinct from both the one for the thermal exponents ν and α of this model, as well as from the analysis for magnetic exponents for other aperiodic model with relevant fluctuations. Figure 7 illustrates the situation for exponents β and γ . They clearly indicate that, for two different choices of (e_2, e_3, e_4) the curves $\frac{d(\log_{10}m)}{d(\log_{10}t)}$ and $\frac{d(\log_{10}\chi)}{d(\log_{10}t)}$ oscillate, with the same frequency ω , about different constant values which represent the actual value of the critical exponents. The quality of the shown data is similar to the one for ξ .

Table 2 also indicates that the magnetic exponents vary along the different directions in the (e_2, e_3, e_4) space, and that they remain invariant by two inversion symmetry operations with respect to both $e_2 \rightarrow -e_2$ (lines 5–7) and $e_3 \rightarrow -e_3$ (lines 3–4). However this does not occur in relation to e_4 (lines 8–9). Test for the accuracy of the results can be obtained by the Rushbrook relation. Table 2 also shows that it is satisfied for all investigated values for (e_2, e_3, e_4) . This strongly supports the claims for a break of universality for Rudin-Shapiro aperiodic model.

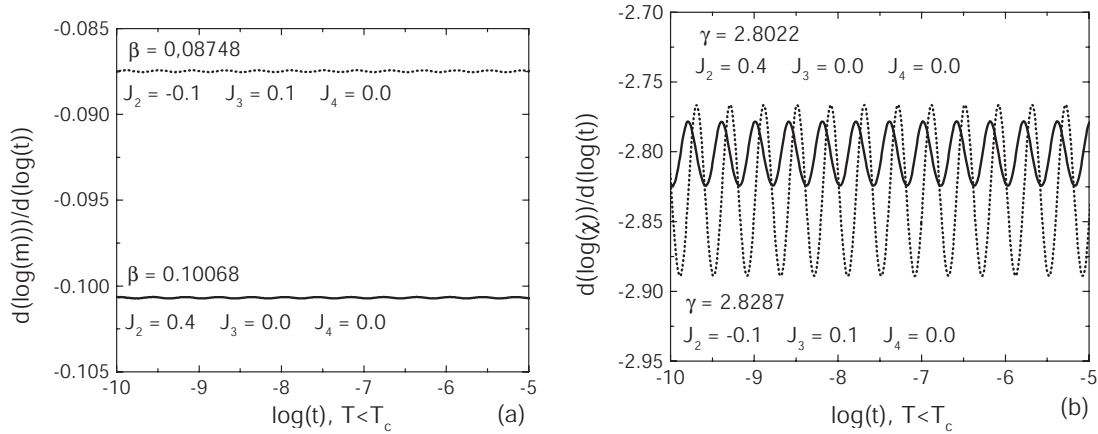


Fig. 7. Plots of $\frac{d(\log_{10} m)}{d(\log_{10} t)}$ (a) and $\frac{d(\log_{10} X)}{d(\log_{10} t)} \times \log_{10} t$ (b) for the same values of (e_2, e_3, e_4) as in the Figure 6. The curves now oscillate about two different horizontal values, indicating distinct values of β and γ .

6 Conclusions

In this paper we analyzed, with great detail, the behavior of the Rudin-Shapiro aperiodic Ising model on the DHL. Several results give a consistent picture for the thermodynamical and critical behavior of the model.

Our results explicitly confirm that, for almost all choices of values of the coupling constants, the model with Rudin-Shapiro aperiodicity brings the model out of the universality class of the uniform model. The exception refers to choices for the constants along the direction of one vanishing eigenvector of the substitution matrix that gives rise to periodic sequences. The new critical behavior is described by an off diagonal *CFP*. We further localized 7 non-critical, unstable period-two cycles, and one off diagonal, fully unstable fixed point. All invariant sets have one vanishing eigenvalue, that is related to the emergence of a periodic sequence.

The critical based on the off diagonal *CFP* contrasts with that obtained for similar aperiodic models on DHL with relevant fluctuations, where [13] the new critical behavior of the aperiodic is governed by a period-two cycle. The MKR analysis included the characterization of a higher than one dimensional invariant manifold linking the critical points of the uniform and aperiodic model. Its localization followed the iteration of the forward and backward MKR maps.

The results based on the MKR analysis were extended by the direct evaluation of the free energy and its derivatives within the TM method, indicating that the critical behavior is indeed controlled by the *CFP*. The TM results shows that the frequency of log periodic oscillations close to T_c , as evaluated by the simple formal solution (19) misses a factor 1/2. This is related to the presence of a negative eigenvalue Λ_2 , the influence of which is not included in that equation.

The TM analysis uncovered a very subtle break of universality which affects the magnetic critical behavior only. The exponents β and γ seem to vary continuously for different directions in the (e_2, e_3, e_4) space. However the Rushbrook and hyper-scale relations are always verified. A

possible explanation for this unusual behavior is found in the MKR analysis: one attractive eigenvector of the *CFP* is associated to a very slow dynamics, as the absolute value of its corresponding eigenvalue is very close to 1. Although we can not indicate the presence of a marginal operator, this very slow dynamics can suffer the influence of external fields that destroys the universal behavior.

The authors are much indebted to T.A. Haddad, S.G. Coutinho and S.R. Salinas for helpfully discussions and suggestions. The work was partially supported by CNPq.

References

1. U. Grimm, M. Baake, *Aperiodic Ising models in The Mathematics of Long-Range Aperiodic Order*, edited by R.V. Moody (Kluwer Academic Publishers, Amsterdam, 1997), pp. 199–237
2. S.T.R. Pinho, T.C.P. Lobão, *Braz. J. Phys.* **30**, 772 (2000)
3. S. Ostlund, R. Pandit, D. Rand, H.J. Schellnhuber, E.D. Siggia, *Phys. Rev. Lett.* **50**, 1873 (1983)
4. J.M. Luck, *Europhys. Lett.* **24**, 359 (1993); *J. Stat. Phys.* **72**, 417 (1993)
5. S.T.R. Pinho, T.A.S. Haddad, S.R. Salinas, *Braz. J. Phys.* **27**, 567 (1997)
6. S.T.R. Pinho, T.A.S. Haddad, S.R. Salinas, *Physica A* **257**, 515 (1998)
7. A.N. Berker, S. Ostlund, *J. Phys. C* **12**, 4961 (1979)
8. M. Kaufman, R.B. Griffiths, *Phys. Rev. B* **24**, 496 (1981)
9. C. Tsallis, A.C.N. de Magalhães, *Phys. Rep.* **268**, 305 (1996)
10. J.M. Yeomans, *Statistical Mechanics of Phase Transitions* (Clarendon Press, Oxford, 1992)
11. D. Sornette, *Rep. Phys.* **297**, 239 (1998)
12. E. Nogueira Jr., R.F.S. Andrade, S. Coutinho, *Eur. Phys. J. B* **23**, 373 (2001)
13. T.A.S. Haddad, S.T.R. Pinho, S.R. Salinas, *Phys. Rev. E* **61**, 3330 (2000)
14. B. Derrida, *J. Phys. A* **16**, 893 (1983)
15. B. Derrida, *J. Stat. Phys.* **33**, 559 (1983)
16. R.F.S. Andrade, *Phys. Rev. E* **59**, 150 (1999)